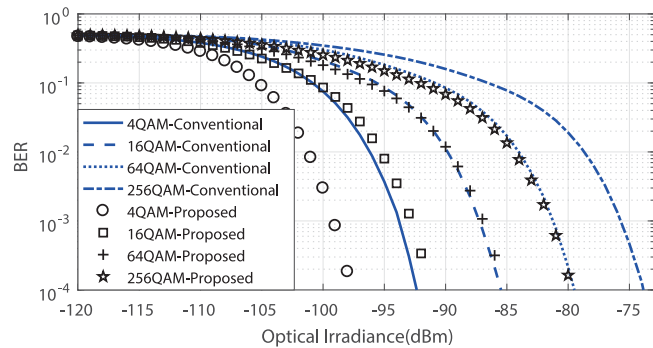


Anscombe Root DCO-OFDM for SPAD-Based Visible Light Communication

Volume 10, Number 2, April 2018

Ying-Dong Zang
Jian Zhang
Ling-Han Si-Ma



DOI: 10.1109/JPHOT.2017.2785798
1943-0655 © 2017 IEEE

Anscombe Root DCO-OFDM for SPAD-Based Visible Light Communication

Ying-Dong Zang , Jian Zhang, and Ling-Han Si-Ma

National Digital Switching System Engineering and Technological Research Center,
Zhengzhou 450000, China

DOI:10.1109/JPHOT.2017.2785798

1943-0655 © 2017 IEEE. Translations and content mining are permitted for academic research only.
Personal use is also permitted, but republication/redistribution requires IEEE permission.
See http://www.ieee.org/publications_standards/publications/rights/index.html for more information.

Manuscript received December 2, 2017; revised December 13, 2017; accepted December 17, 2017.
Date of publication January 23, 2018; date of current version April 6, 2018. Corresponding author:
Ying-Dong Zang (e-mail: zangyingdong@126.com).

Abstract: For high-speed visible light communication (VLC) with weak signals such as in underwater environment, dc-biased optical orthogonal frequency-division multiplexing (DCO-OFDM) based on single-photon avalanche diodes (SPADs) is viewed as a promising scheme. Since the channel noise is Poisson distributed, the maximum likelihood (ML) detection is mathematically intractable for DCO-OFDM, and the ML-detection-based minimum distance criterion originally for Gaussian channels is applied to SPAD-based DCO-OFDM. However, the error performance is degraded. For this reason, we propose an Anscombe root (AR) DCO-OFDM by using the existing AR transformation before fast Fourier transformation at the receiver side and a square operation at the transmitter. For the proposed AR-DCO-OFDM, the channel noise is well approximated to be Gaussian distributed, and thus, the asymptotically optimal detection is based on the low-complexity minimum-distance criterion. Extensive simulations indicate that our proposed AR-DCO-OFDM can substantially improve the conventional DCO-OFDM with minimum-distance detection for SPAD-based VLC systems, and the attained gain is above 5 dB at the bit error rate of 10^{-4} for numerous scenarios.

Index Terms: Visible light communication, OFDM, single photon avalanche diodes (SPADs), Anscombe root transformation and maximum likelihood.

1. Introduction

Recently, visible light communication (VLC) based on light emitting diodes (LEDs) has received extensive attention for the advantages such as license-free, cost-effective, high security and immunity to electromagnetic comparing to traditional radio frequency (RF) [1]–[5]. A typical VLC system usually use photodiodes (PDs) as receivers. However, PDs are not sensitive enough to detect the weak optical signal such as in underwater optical wireless communication (UOWC). In UOWC, the optical signal usually suffers from absorption, scattering and turbulence during the transmission in the water and thus, becomes weak sharply [6]. Therefore, a high sensitive detector, single photon avalanche diodes (SPADs), is proposed for such weak illuminance applications to achieve a long-range communication [7]. For high-speed wireless communications, multiple carrier modulation such as orthogonal frequency division multiplexing (OFDM) is applied to SPAD-based VLC [8].

Unfortunately, OFDM for SPAD-based VLC has two significant technical difference from the OFDMs for conventional OFDM RF communications and that for PD-based VLC. On one hand, OFDM employed in radio frequency RF communications can be used in VLC due the nonnegativity requirement of intensity modulation [9]. For this reason, Hermitian symmetry of optical OFDM

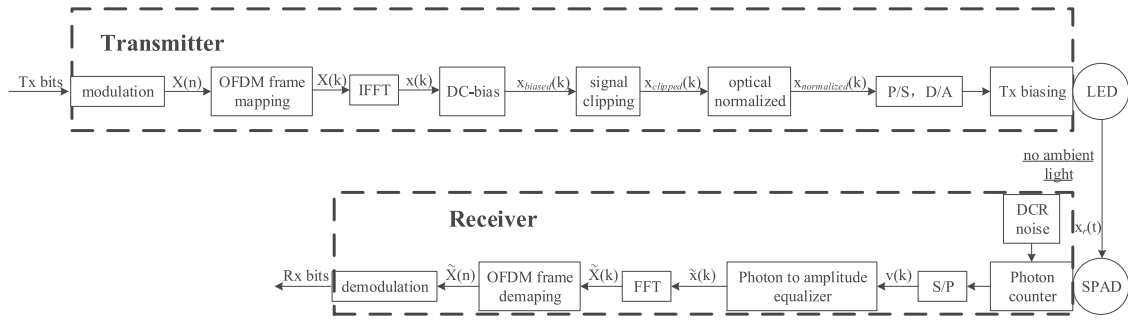


Fig. 1. Conventional SPAD-OFDM system.

symbols before the inverse fast Fourier transform (IFFT) operation is employed for obtaining real-valued symbols, meanwhile, DC-bias or asymmetrically clipped operation is used for generating the nonnegative signal. Asymmetrically clipped optical OFDM (ACO-OFDM) and DC-biased optical OFDM (DCO-OFDM) are two commonly used schemes [10]–[13]. Since the spectral efficiency of DCO-OFDM is twice that of ACO-OFDM [14], in this paper, we consider DCO-OFDM. On the other hand, SPAD usually works in Poisson regimes and the corresponding channel noise is Poisson-distributed [15], [16]. In RF or PD-based OFDM, where the additive noise is Gaussian-distributed, the noise after FFT is still Gaussian. Therefore, the optimal maximum likelihood (ML) detection is equivalent to the minimum distance decision. Unfortunately, for the SPAD-based DCO-OFDM, the likelihood function of the FFT output is mathematically intractable and thus, the ML detection is very complicated. For this reason, the authors in [8] proposed to use the minimum distance detection. Although this detection complexity is very low, the error performance is degraded since the channel noise is not Gaussian yet. We also notice that the authors in [17] proposed a powerful technique based on Anscombe root (AR) transformation [18], [19] to process the signal detection over Poisson channels. However, the low-complexity detection for DCO-OFDM with enhanced performance remains open up to now.

Therefore, the aforementioned factors indeed motivate us to propose a new form of DCO-OFDM, which is called AR-DCO-OFDM by applying AR transformation to the conventional DCO-OFDM [8] to approximating the resulting Poisson channels into a Gaussian channels without significantly increasing the detection complexity. Simulations indicate that our proposed AR-DCO-OFDM can substantially outperform the conventional DCO-OFDM for SPAD-based UOWC systems proposed in [8].

2. Conventional DCO-OFDM

To make our idea of AR-DCO-OFDM as clear as possible, in this section we mainly introduce the details of the conventional DCO-OFDM for SPAD-based VLC recently proposed in [8].

2.1 Transmitter

For DCO-OFDM shown by Fig. 1, the input bit stream is modulated into M -ary quadrature amplitude modulation (QAM) symbols, where M denotes the modulation order. Then, the QAM symbols are transformed by a size- N inverse fast Fourier transformation (IFFT), generating $X(k)$, $0 \leq k \leq N - 1$. For VLC, the intensity modulation requires the transmitted signals of LED to be nonnegative and real-valued. Therefore, the following successive steps are needed.

2.1.1 Hermitian Symmetry: To satisfy the real-valued required, it is required that $X(0) = X(N/2) = 0$ and a Hermitian symmetry is guaranteed, say,

$$X(k) = X^*(N - k), \frac{N}{2} + 1 \leq k \leq N - 1, \quad (1)$$

where X^* denote the conjugate of X .

2.1.2 Adding DC: To make a proper range of the signal amplitude be nonnegative, some DC-bias should be added to $X(k)$. According to the results in [20], the DC-bias can be usually computed by

$$B_{DC} = \alpha \sqrt{E\{x^2(k)\}}, \quad (2)$$

where α is a given constant and the level of DC can be valued by $10 \log_{10}(\alpha^2 + 1)$ in dB. In this way, the DC-bias is variable with the signal. Then, we get $x_{biased}(k) = x(k) + B_{DC}$. It should be mentioned that the DC-bias added here is used to make the signal nonnegative basically and it is different from the Tx biasing used in Fig. 1. The Tx biasing is used to make the LED work in its linear range.

2.1.3 Signal Clipping: However, since the peak-to-average ratio of OFDM signals, $x_{biased}(k)$, is quite high, it is hard to make all the amplitude of signals nonnegative. For this reason, a signal clipping will be adopted in the following

$$x_{clipped}(k) = \frac{1}{2}(x_{biased}(k) + |x_{biased}(k)|), \quad (3)$$

where $0 \leq k \leq N - 1$.

2.2 Receiver

At the receiver side of DCO-OFDM, an SPAD array, which is an APD in the Geiger mode [21], is used to count the received photons. This process of the photons arriving at an SPAD array could be modelled as a standard counting process [8]. Then, the output of SPAD can be represented by

$$v(k) = (CT_s/E_p)x_{clipped}(k) + NT_s + p, \quad (4)$$

where $v(k)$ is the photon number counted by an SPAD array, p denotes an additive Poisson noise scalar, C means the photon detection efficiency of the SPAD, N denotes the dark count rate of an SPAD array, E_p is the single photon energy and T_s denotes the time of counting. The probability density functions (PDFs) of $v(k)$ and p could be expressed respectively as

$$\begin{cases} \Pr(v(k) = n) = e^{-E\{v(k)\}} \frac{E^{-n}\{v(k)\}}{n!} \\ \Pr(p = n) = e^{-E\{v(k)\}} \frac{E^{-(n+E\{v(k)\})}\{v(k)\}}{(n+E\{v(k)\})!}, \end{cases} \quad (5)$$

where $E\{v(k)\} = (CT_s/E_p)x_{clipped}(k) + NT_s$.

Then, the SPAD output is transformed into electrical signal by an equalizer [8], [22], followed by an FFT operation, whose output is denoted by $\tilde{X}(n)$. Because of Hermitian symmetry, we are only interested in $\tilde{X}(n)$, $1 \leq n \leq N/2 - 1$ [20]. In the RF OFDM or PD-based OFDM, where the channel noise is white Gaussian distributed, the optimal maximum likelihood (ML) detection follows the minimum Euclidean decision, whose complexity is very low. Unfortunately, for DCO-OFDM based on SPAD, the channel noise is Poisson-distributed. Frankly speaking, the corresponding likelihood function of the Poisson noise after FFT is mathematically intractable and there is not an optimal ML detection for SPAD-based DCO-OFDM yet. Therefore, the authors in [8] proposed to use the conventional minimum Euclidean distance detection. As expected, the resulting error performance is degraded.

In this paper, our main task is to develop a new DCO-OFDM for SPAD-based VLC with an enhanced error performance and low-complexity detection.

3. Proposed AR-DCO-OFDM

In this section, our primary purpose is to develop an AR-DCO-OFDM. The main idea is to add a non-linear transformation and its inverse to the conventional DCO-OFDM presented in Section II.

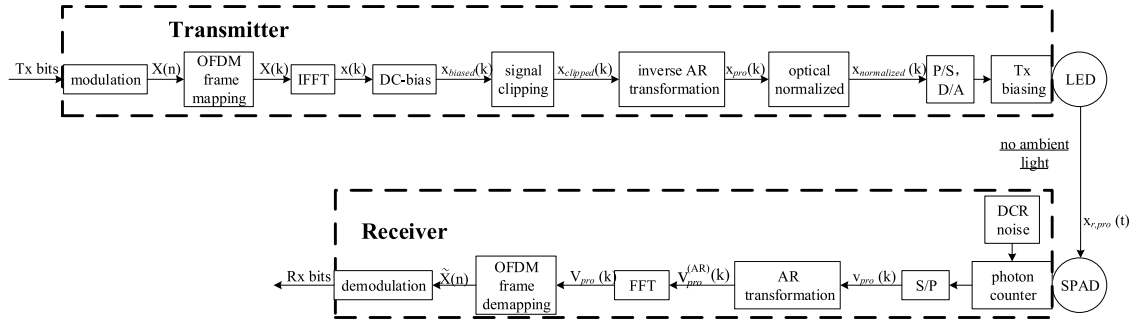


Fig. 2. Proposed SPAD-OFDM system.

3.1 Anscombe Root Transformation

Let us briefly introduce the AR transformation. Given a random variable z obeying the Poisson distribution, the AR transformation of z can be expressed as [18], [19]

$$z^{(AR)} = \sqrt{z + 3/8}. \quad (6)$$

According to [18], [19], the variance of $z^{(AR)}$, $D\{z^{(AR)}\}$, is approximated by

$$D\{z^{(AR)}\} \approx \frac{1}{4} \left(1 + \frac{1}{16E^2\{z\}} \right). \quad (7)$$

In addition, from the fact that $D\{x\} = E\{x^2\} - E^2\{x\}$ for any random variable x and (7), we can obtain

$$E\{z^{(AR)}\} \approx \sqrt{E\{z\} + \frac{1}{8} - \frac{1}{64E^2\{z\}}}. \quad (8)$$

According to [19], when $E\{z\}$ is large enough, $z^{(AR)}$ can be well approximated by Gaussian-distributed variable with $E\{z^{(AR)}\} \approx \sqrt{E\{z\}}$. Thus, we can attain

$$z^{(AR)} = \sqrt{z + \frac{3}{8}} \approx \sqrt{E\{z\}} + \zeta, \quad (9)$$

where ζ is an approximate additive Gaussian noise. The author in [19] employ Taylor series expansion to the (6) and analyzed the Lagrange' form of the remainder term. It reveals that when $E\{z\}$ is large enough, ζ will has zero mean with an approximate variance being 0.25. There are exhaustive details in the second page of [19] and we won't explore it in this article. The author in [18] also had make tables and draw the curves to show the result directly.

3.2 AR-DCO-OFDM

In [17], the existing AR transformation [18], [19] was shown to be a powerful tool for the low-complexity signal detection in the Poisson noise channels of SPAD-based VLC. Motivated by [17], we apply AR to the DCO-OFDM to attain a better performance than the minimum distance based DCO-OFDM by applying AR transformation to $v(k)$ at the receiver and its approximated inverse at the transmitter. With AR and its inverse, the corresponding signal recovery is similar to that of Gaussian noise channels. Now, we formally state our proposed AR-DCO-OFDM.

3.2.1 Transmitter: For our proposed AR-DCO-OFDM shown by Fig. 2, we transform the clipping processing output, $x_{clipped}(k)$, in the following

$$x_{pro}(k) = x_{clipped}^2(k) \quad (10)$$

which is approximately viewed as the inverse AR transformation.

3.2.2 Receiver: For convenience, we denote that output of SPAD by $v_{\text{pro}}(k)$. Then, according to (9), the AR-version of $v_{\text{pro}}(k)$ can be

$$\begin{aligned} v_{\text{pro}}^{(\text{AR})}(k) &= \sqrt{v_{\text{pro}}(k) + 3/8} \\ &= \sqrt{(CT_s/E_p)x_{\text{pro}}(k) + NT_s + p + 3/8} \\ &\approx \sqrt{(CT_s/E_p)x_{\text{pro}}(k) + NT_s} + \zeta(k). \end{aligned} \quad (11)$$

When the optical intensity is sufficiently high, say, $v_{\text{pro}}(k) \gg NT_s$, the constant NT_s can be ignored. In other words, we further approximate $v_{\text{pro}}^{(\text{AR})}(k)$ by

$$v_{\text{pro}}^{(\text{AR})}(k) \approx \sqrt{(CT_s/E_p)x_{\text{pro}}(k)} + \zeta(k). \quad (12)$$

3.2.3 Low-Complexity Detection: After AR processing, $v_{\text{pro}}^{(\text{AR})}(k)$ is fed to FFT processing, yielding $V_{\text{pro}}(n)$,

$$\begin{aligned} V_{\text{pro}}(n) &= \text{FFT}\left[v_{\text{pro}}^{(\text{AR})}(n)\right] \\ &\approx \text{FFT}\left[\sqrt{(CT_s/E_p)x_{\text{pro}}(n)}\right] + \text{FFT}[\zeta(n)] \\ &= \text{FFT}\left[\sqrt{(CT_s/E_p)}x_{\text{clipped}}(n)\right] + \text{FFT}[\zeta(n)] \end{aligned} \quad (13)$$

where $x_{\text{pro}}(k) = x_{\text{clipped}}^2(k)$ defined in (10), $\text{FFT}[x]$ denotes the FFT output for x and $0 \leq n \leq N - 1$. Again, from the Hermitian symmetry property, we estimate the transmitted message from $V_{\text{pro}}(n)$, where $1 \leq k \leq N/2 - 1$. In addition, from the property of AR transformation and the fact that $\text{FFT}[\zeta(n)]$ is an orthogonal transform of $\zeta(n)$, $\text{FFT}[\zeta(n)]$ is still a Gaussian random variable. Therefore, we can use the well-known minimum distance criterion to estimate the transmitted signals. These important observations lead us to the following low-complexity detection mechanism for our proposed AR-DCO-OFDM.

Detection for AR-DCO-OFDM: Given the received signal $v_{\text{pro}}(k)$, $k = 1, 2, \dots, N$, the detection for AR-DCO-OFDM is attained by the following successive steps:

- 1) *AR transformation:* $v_{\text{pro}}^{(\text{AR})}(k) = \sqrt{v_{\text{pro}}(k) + 3/8}$.
- 2) *FFT Operation:* $V_{\text{pro}}(n) = \text{FFT}[v_{\text{pro}}^{(\text{AR})}(n)]$.
- 3) *Minimum-Distance Demodulation:* Demodulate the transmitted $x(n)$ from $V_{\text{pro}}(n)$ for $1 \leq n \leq N/2 - 1$. ■

It should be noticed that the demodulation complexity is very low for the commonly used QAM since the complexity is equivalent to that of an integer quantization.

4. Simulation Results

In this section, we examine the error performance of our proposed AR-DCO-OFDM by comparing with the conventional DCO-OFDM in [8]. Throughout the simulation, the detailed parameter set is showed in Table 1.

Since the AR transform is non-linear, we first present the approximation performance with respect to the PDF of $v_{\text{pro}}^{(\text{AR})}(k) - \sqrt{(CT_s/E_p)x_{\text{pro}}(k)}$. According to (9), the PDF of ζ is represented by $f(x) = \sqrt{2/\pi} \exp(-2x^2)$. Figs. 3 and 4 show the comparison between the theory curve given by $f(x) = \sqrt{2/\pi} \exp(-2x^2)$ and the simulation results for DCO-OFDM of 64-QAM with 13 dB-bias and different optical irradiance. In the simulations, we consider the channel with no attenuation. For the receiving optical signal is weak for SPAD, we set the given optical irradiance in dBm level. And we employ transmitting optical irradiance normalization as the comparison standard in the simulations. For the

TABLE 1
Simulation Parameters

Single photon energy (E_p) [21]	4.42×10^{-19} J
The PDE of the SPAD (C) [21]	20%
The DCR of the SPAD array (N_{DCR}) [21]	7.27 kHz
Time interval of a symbol (T_s) [21]	1 ms
The size of the SPAD array [21]	1024
The size of the FFT/IFFT (N)	2048

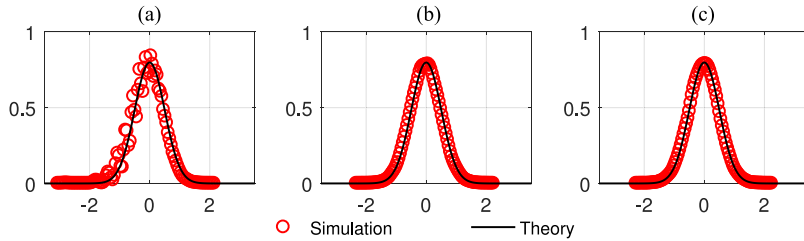


Fig. 3. Noise PDF comparison.

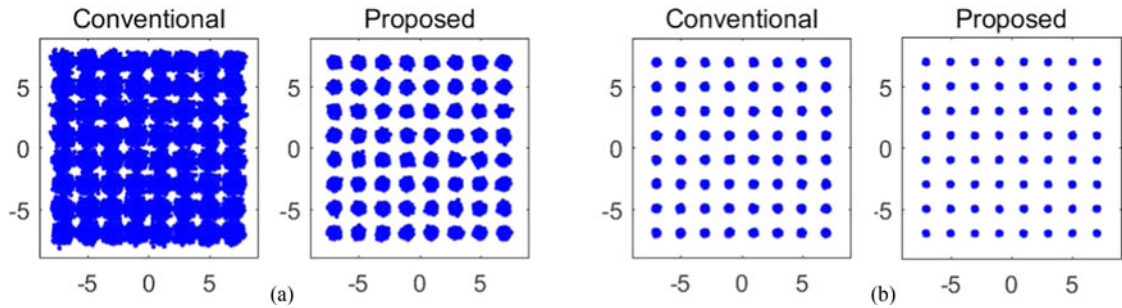


Fig. 4. Received constellation comparison. (a) -80 dBm comparison. (b) -70 dBm comparison.

conventional system in Fig. 1, the normalization would be

$$x_{\text{normalized}}(k) = \frac{x_{\text{clipped}}(k)}{\mathbb{E}\{x_{\text{clipped}}(k)\}}. \quad (14)$$

For the proposed system in Fig. 2, the normalization would be

$$x_{\text{normalized}}(k) = \frac{x_{\text{pro}}(k)}{\mathbb{E}\{x_{\text{pro}}(k)\}}. \quad (15)$$

For typical digital communication system, the digital-to-analog converter (DAC) usually has a limited dynamic range. In this paper, we assume that the dynamic range is large enough and won't make a high boundary clipping to the signal. Then, the $x_{\text{normalized}}$ is transmitted by the LED with different given average transmitting optical irradiance. It should be noticed that the DC is a function of the signal and is not relevant to the average transmitting optical irradiance given here. In this paper, we focus on the performance comparison between the conventional SPAD-based DCO-OFDM system in [8] and our proposed system. Therefore, we employ the same setting of the channel that the optical signals arrive the SPADs over a long distance in the absence of background light. Thus, the

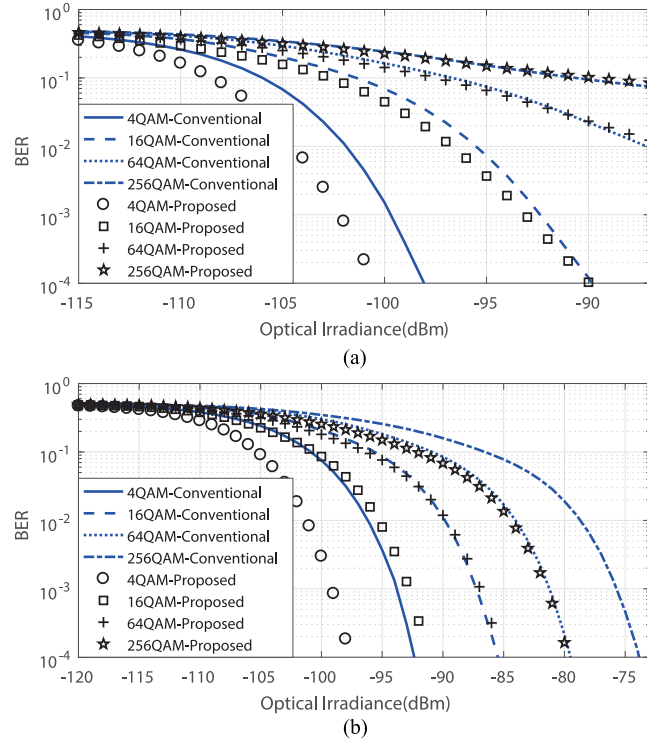


Fig. 5. Comparison between the conventional and the proposed systems for given dc bias. (a) dc bias: $10\log_{10}(\alpha^2 + 1) = 7$ dB, $\alpha = 2$. (b) dc bias: $10\log_{10}(\alpha^2 + 1) = 13$ dB, $\alpha = 4.3535$.

optical signals are assumed to pass through a flat fading channel and to be distorted by the shot noise. Fig. 3 shows that, with increasing average transmitting optical irradiance, the PDF of the simulation data approaches that of ζ . In addition, from Fig. 4 illustrating the constellation diagrams for AR-DCO-OFDM and the conventional DCO-OFDM, we can observe that the constellation of our proposed AR-DCO-OFDM has a larger signal-noise ratio. Therefore, from the above two figures, it is reasonable to expect that the error performance of AR-DCO-OFDM outperforms that of the conventional one in [8], which will be verified by the following simulation results.

In the following, we compare the average bit error rate (BER) performance of AR-DCO-OFDM and the conventional DCO-OFDM and show the simulations in Figs. 5 and 6. Fig. 5 presents the error performance of different M with $10\log_{10}(\alpha^2 + 1) = 7, 13$, which are the typical values given by [8], [20]. As illustrated by Fig. 5, for the same M and α , substantial gain can be attained by AR-DCO-OFDM over the conventional DCO-OFDM. For example, when $M = 4$ and $10\log_{10}(\alpha^2 + 1) = 13$, the attained gain is about 5 dB at the BER of 10^{-4} . Furthermore, for a fixed modulation order, we show the error performance comparison for different α in Fig. 6. From this figure, we observe that for the presented α , our AR-DCO-OFDM has lower BER for the same transmitted power. For example, when $M = 64$ and $10\log_{10}(\alpha^2 + 1) = 13$, the performance gain is above 5 dB. In addition, we can see that a proper DC selection is of much significance for a satisfactory performance since if the values of α is too small or too large, the performance will be degraded. For instance, when $M = 64$ and $10\log_{10}(\alpha^2 + 1) = 7$, there exists an error floor, for which the main reason is that when α is too small, the distortion resulting from the clipping processing of nonnegative components will worsen the error performance. If α is too large, the energy-efficiency is not guaranteed as indicated by the case of $M = 64$ and $10\log_{10}(\alpha^2 + 1) = 16$. Therefore, a proper trade-off with respect to α is required. It is a crucial topic and we will consider it in our future research.

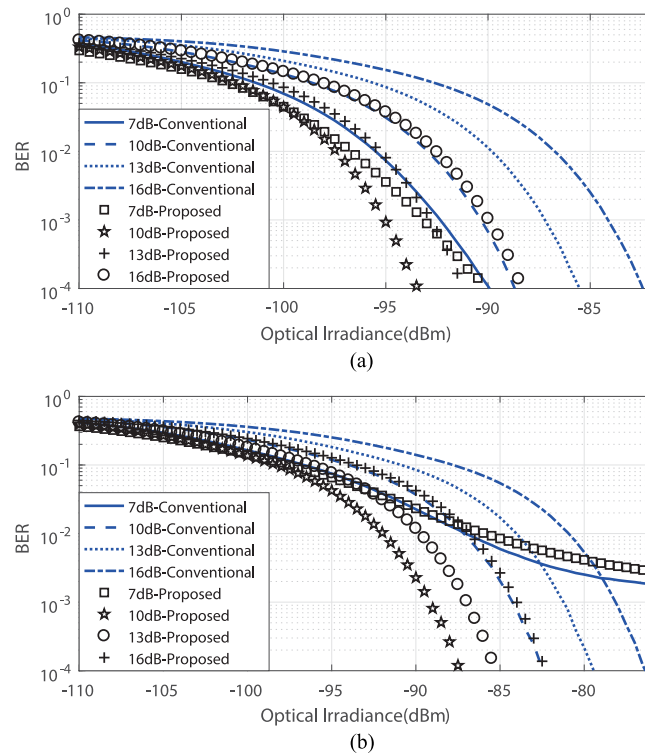


Fig. 6. Comparison between the conventional and the proposed systems for given constellation size.
 (a) 16-QAM. (b) 64-QAM.

5. Conclusion

In this paper, we have proposed AR-DCO-OFDM for SPAD-based VLC systems by using the existing AR transformation at the receive side and a square operation at the transmitter. The resulting noise of the proposed AR-DCO-OFDM has been shown to be well approximated by a Gaussian random variable. This important property allows us to demodulate the transmitted signals by using the low-complexity minimum Euclidean distance demodulation. Comprehensive simulation results have shown that our proposed AR-DCO-OFDM has substantial performance gain over the conventional scheme.

References

- [1] N. Kumar and N. R. Lourenco, "LED-based visible light communication system: A brief survey and investigation," *J. Eng. Appl. Sci.*, vol. 5, pp. 297–307, 2010.
- [2] Y. Y. Zhang, H. Y. Yu, J. K. Zhang, Y. J. Zhu, J. L. Wang, and T. Wang, "Space codes for MIMO optical wireless communications: Error performance criterion and code construction," *IEEE Trans. Wireless Commun.*, vol. 16, no. 5, pp. 3072–3085, May 2017.
- [3] Y. Y. Zhang, H. Y. Yu, J. K. Zhang, Y. J. Zhu, J. L. Wang, and X. S. Ji, "On the optimality of spatial repetition coding for MIMO optical wireless communications," *IEEE Commun. Lett.*, vol. 20, no. 5, pp. 846–849, May 2016.
- [4] Y. Y. Zhang, H. Y. Yu, J. K. Zhang, and Y. J. Zhu, "Signal-cooperative multilayer-modulated VLC systems for automotive applications," *IEEE Photon. J.*, vol. 8, no. 1, Feb. 2016, Art. no. 6800509.
- [5] Y. Y. Zhang, H. Y. Yu, and J. K. Zhang, "Block precoding for peak-limited MISO broadcast VLC: Constellation-optimal structure and addition-unique designs," *IEEE J. Sel. Areas Commun.*, 2017, to be published.
- [6] M. V. Jamali and J. A. Salehi, "On the BER of multiple-input multiple-output underwater wireless optical communication systems," in *Proc. Int. Workshop Opt. Wireless Commun.*, 2015, pp. 26–30.
- [7] X. Liu, C. Gong, S. Li, and Z. Xu, "Signal characterization and receiver design for visible light communication under weak illuminance," *IEEE Commun. Lett.*, vol. 20, no. 7, pp. 1349–1352, Jul. 2016.

- [8] Y. Li, M. Safari, R. Henderson, and H. Haas, "Optical OFDM with single-photon avalanche diode," *IEEE Photon. Technol. Lett.*, vol. 27, no. 9, pp. 943–946, May 2015.
- [9] J. Armstrong, "OFDM for optical communications," *J. Lightw. Technol.*, vol. 27, no. 3, pp. 189–204, Feb. 2009.
- [10] J. Armstrong and A. J. Lowery, "Power efficient optical OFDM," *Electron. Lett.*, vol. 42, no. 6, pp. 370–372, 2006.
- [11] Y. Gao, J. Yu, J. Xiao, Z. Cao, F. Li, and L. Chen, "Direct-detection optical OFDM transmission system with pre-emphasis technique," *J. Lightw. Technol.*, vol. 29, no. 14, pp. 2138–2145, Jul. 2011.
- [12] J. Zhou, Y. Yan, Z. Cai, and Y. Qiao, "A cost-effective and efficient scheme for optical OFDM in short-range IM/DD systems," *IEEE Photon. Technol. Lett.*, vol. 26, no. 13, pp. 1372–1374, Jul. 2014.
- [13] J. Zhou and Y. Qiao, "Low-PAPR asymmetrically clipped optical OFDM for intensity-modulation/direct-detection systems," *IEEE Photon. J.*, vol. 7, no. 3, Jun. 2015, Art. no. 7101608.
- [14] S. D. Dissanayake and J. Armstrong, "Comparison of ACO-OFDM, DCO-OFDM and ADO-OFDM in IM/DD systems," *J. Lightw. Technol.*, vol. 31, no. 7, pp. 1063–1072, Apr. 2013.
- [15] S. Karp and J. Clark, "Photon counting: A problem in classical noise theory," *IEEE Trans. Inf. Theory*, vol. IT-16, no. 6, pp. 672–680, Nov. 1970.
- [16] M. C. Teich and S. Rosenberg, "Photocounting array receivers for optical communication through the lognormal atmospheric channel 2: Optimum and suboptimum receiver performance for binary signaling," *Appl. Opt.*, vol. 12, no. 11, pp. 2625–2635, 1973.
- [17] J. Zhang, L. H. Si-Ma, B. Q. Wang, J. K. Zhang, and Y. Y. Zhang, "Low-complexity receivers and energy-efficient constellations for SPAD VLC systems," *IEEE Photon. Technol. Lett.*, vol. 28, no. 17, pp. 1799–1802, Sep. 2016.
- [18] M. S. Bartlett, "The square root transformation in analysis of variance," *J. Roy. Statist. Soc.*, vol. 3, no. 1, pp. 68–78, 1936.
- [19] P. H. Leslie, "The transformation of Poisson, binomial and negative-binomial data," *Biometrika*, vol. 35, nos. 3/4, pp. 246–254, 1948.
- [20] J. Armstrong and B. Schmidt, "Comparison of asymmetrically clipped optical OFDM and DC-biased optical OFDM in AWGN," *IEEE Commun. Lett.*, vol. 12, no. 5, pp. 343–345, May 2008.
- [21] E. Fisher, I. Underwood, and R. Henderson, "A reconfigurable single-photon-counting integrating receiver for optical communications," *IEEE J. Solid-State Circuits*, vol. 48, no. 7, pp. 1638–1650, Jul. 2013.
- [22] Y. Li, M. Safari, R. Henderson, and H. Haas, "Nonlinear distortion in SPAD-based optical OFDM systems," in *Proc. IEEE GLOBECOM Workshops*, 2015, pp. 1–6.